Journal of Mathematical Chemistry 26 (1999) 243–254

Scalar wave diffraction from zero-range scatterers

Radosław Szmytkowski and Czesław Szmytkowski

Atomic Physics Division, Faculty of Applied Physics and Mathematics, Technical University of Gdańsk, ul. Narutowicza 11/12, PL 80-952 Gdańsk, Poland

Received 17 August 1999

The zero-range approximation for wave scattering is popularized. The general idea of the approximation is outlined and the theory is applied to solve an illustrative example: diffraction on a system of four identical scatterers forming a T_d-symmetry structure. The group theoretical methods are used to decompose a scattered wave into four partial waves adequate to the symmetry group of the target. Concepts of partial scattering amplitudes, associated phase shifts and partial cross sections for the nonspherical target considered are introduced and utilized. It is shown that under some conditions a phenomenon of resonant scattering may occur.

1. Introduction

Problems of wave scattering from discrete systems of obstacles are frequently considered in applications of the theory of wave motion. They are met, for instance, in atomic, molecular, chemical, condensed matter and nuclear science as well as in acoustics, electromagnetic theory and geophysics. A solution to any particular problem depends on physical nature of a wave and targets, on laws of their interaction, on size and shape of individual obstacles, their relative localization and on wave length. Such a variety of factors which should be taken into account causes that in most cases only numerical solutions are available. Obviously, analytical solutions, even approximate, always remain of considerable interest because of their compactness and a possibility they offer to discuss the dependency of scattering observables on parameters characterizing a system.

An interesting and useful approximate analytical method of solving the problem of wave diffraction on a system of targets in the extreme case when spatial dimensions of individual scatterers are much lesser than the wave length was developed by nuclear physicists [2]. The method, known as *the zero-range approximation*, bases on the assumption that scatterers may be considered to be point-like and that their interaction with the wave may be modeled by a set of limiting conditions obeyed by a solution of a wave equation at points where these zero-range scatterers are situated. Until now the approximation has found numerous applications in quantum theory [2,5–9,12 and references therein]. It is a purpose of this paper to popularize the zero-range approximation by showing its ability to provide analytical solutions to diffraction problems of interest for chemists and molecular physicists.

The rest of the work is divided into two sections. Section 2 contains a brief outline of the theory of wave scattering from an arbitrary system of zero-range targets. In section 3 wave diffraction from a system of four identical zero-range scatterers located in vertices of a fictitious regular tetrahedron is considered as an example of the applicability of the zero-range approximation. A scattered wave is decomposed into partial waves adequate to the T_d-symmetry point group to which the target belongs. Concepts of partial scattering amplitudes, associated phase shifts and partial cross sections for such a nonspherical scatterer are then introduced and applied. The section concludes with showing that under some conditions wave scattering from the obstacle under study may be of a resonant character.

2. Diffraction from zero-range scatterers: an outline of the theory

Consider situation when a scalar plane wave of the wave vector $\boldsymbol{k}_i$ impinges on a system consisting of N fixed, in general non-identical, zero-range non-absorbing spherically symmetric obstacles located at points $\boldsymbol{r}_n$, $n = 1, \ldots, N$. Everywhere, except the points where the scatterers are situated, the time-independent wave equation is the Helmholtz equation

$$\left[\boldsymbol{\nabla}^2 + k^2\right]\Psi(\boldsymbol{k}_i, \boldsymbol{r}) = 0 \quad (\boldsymbol{r} \neq \boldsymbol{r}_n, n = 1, \ldots, N), \tag{1}$$

where $k = |\boldsymbol{k}_i|$. Its particular solution, describing the process under consideration, has the form

$$\Psi(\boldsymbol{k}_i, \boldsymbol{r}) = \mathrm{e}^{\mathrm{i}\boldsymbol{k}_i \cdot \boldsymbol{r}} + \Phi(\boldsymbol{k}_i, \boldsymbol{r}), \tag{2}$$

in which the first and the second term on the right represents the incident and the scattered wave, respectively. It is assumed that the scattered wave $\Phi(\boldsymbol{k}_i, \boldsymbol{r})$ is a superposition of N spherically symmetric waves outgoing from individual targets

$$\Phi(\boldsymbol{k}_i, \boldsymbol{r}) = \sum_{n=1}^{N} f_n(\boldsymbol{k}_i)\phi_n(\boldsymbol{r}), \tag{3}$$

where

$$\phi_n(\boldsymbol{r}) = \frac{\mathrm{e}^{\mathrm{i}k|\boldsymbol{r}-\boldsymbol{r}_n|}}{|\boldsymbol{r} - \boldsymbol{r}_n|} \quad (n = 1, \ldots, N), \tag{4}$$

while $f_n(\boldsymbol{k}_i)$ are the superposition coefficients which are to be found. Since the targets are point-like, their interaction with the incident wave, resulting in a formation of the scattered wave, must be given in the form of a set of limiting conditions imposed on the solution of equation (1) at the points where the targets are situated. The particular form of these conditions follows from the assumption that the obstacles do not absorb the wave. This means that the flux of the vector

$$\boldsymbol{j} = \operatorname{Im}\left[\Psi^*(\boldsymbol{k}_i, \boldsymbol{r})\boldsymbol{\nabla}\Psi(\boldsymbol{k}_i, \boldsymbol{r})\right] \tag{5}$$

through an infinitesimal spherical surface centered at an arbitrary scattered vanishes

$$\lim_{\boldsymbol{r}\to\boldsymbol{r}_n} \int_{S_n} \mathrm{d}S_n \frac{\boldsymbol{r}-\boldsymbol{r}_n}{|\boldsymbol{r}-\boldsymbol{r}_n|} \cdot \operatorname{Im}\left[\Psi^*(\boldsymbol{k}_i, \boldsymbol{r})\boldsymbol{\nabla}\Psi(\boldsymbol{k}_i, \boldsymbol{r})\right] = 0 \quad (n = 1, \ldots, N). \tag{6}$$

(The vector $(\boldsymbol{r}-\boldsymbol{r}_n)/|\boldsymbol{r}-\boldsymbol{r}_n|$ is the unit vector normal to the sphere S_n at the point $\boldsymbol{r}$.) It may be verified by direct substitution that the constraint (6) is satisfied if the function $\Psi(\boldsymbol{k}_i, \boldsymbol{r})$ obeys the conditions

$$\lim_{\boldsymbol{r}\to\boldsymbol{r}_n} \left[1 + \kappa_n|\boldsymbol{r}-\boldsymbol{r}_n| + (\boldsymbol{r}-\boldsymbol{r}_n)\cdot\boldsymbol{\nabla}\right]\Psi(\boldsymbol{k}_i, \boldsymbol{r}) = 0 \quad (n = 1, \ldots, N), \tag{7}$$

where κ_n is a real parameter characterizing the nth scatterer. In general, one might consider the possibility that the parameters κ_n, $n = 1, \ldots, N$, are k-dependent but in what follows we shall restrict our analysis to the simplest case when they are constant.

The conditions (7) enable one to find the superposition coefficients in the outgoing wave (3). Indeed, substitution of equations (2) and (3) into equation (7) yields the system of algebraic equations for $f_n(\boldsymbol{k}_i)$

$$(\mathrm{i}k + \kappa_n) f_n(\boldsymbol{k}_i) + \sum_{\substack{m=1 \\ (m \neq n)}}^{N} f_m(\boldsymbol{k}_i)\phi_m(\boldsymbol{r}_n) = -\mathrm{e}^{\mathrm{i}\boldsymbol{k}_i\cdot\boldsymbol{r}_n}, \tag{8}$$

which, at least in principle, may be solved for an arbitrary geometry of the scattering centers. The solution facilitates, however, whenever the target system is invariant under some group of symmetry transformations. This will be illustrated in the next section.

Once the coefficients $f_n(\boldsymbol{k}_i)$ have been found, the scattering amplitude $\mathcal{F}(\boldsymbol{k}_i, \boldsymbol{k}_f)$, defined by

$$\Phi(\boldsymbol{k}_i, \boldsymbol{r}) \overset{r\to\infty}{\longrightarrow} \mathcal{F}(\boldsymbol{k}_i, \boldsymbol{k}_f)\frac{\mathrm{e}^{\mathrm{i}kr}}{r} \tag{9}$$

with $\boldsymbol{k}_f = k\boldsymbol{r}/r$, may be determined. Combining the obvious asymptotic relation

$$\phi_n(\boldsymbol{r}) \overset{r\to\infty}{\longrightarrow} \mathrm{e}^{-\mathrm{i}\boldsymbol{k}_f\cdot\boldsymbol{r}_n}\frac{\mathrm{e}^{\mathrm{i}kr}}{r} \quad (n = 1, \ldots, N) \tag{10}$$

with equations (3) and (9), one obtains

$$\mathcal{F}(\boldsymbol{k}_i, \boldsymbol{k}_f) = \sum_{n=1}^{N} f_n(\boldsymbol{k}_i)\mathrm{e}^{-\mathrm{i}\boldsymbol{k}_f\cdot\boldsymbol{r}_n}. \tag{11}$$

Given the amplitude $\mathcal{F}(\boldsymbol{k}_i, \boldsymbol{k}_f)$, other quantities characterizing the scattering process, such as the differential cross section for the transition $\boldsymbol{k}_i \to \boldsymbol{k}_f$

$$\sigma(\boldsymbol{k}_i, \boldsymbol{k}_f) = \left|\mathcal{F}(\boldsymbol{k}_i, \boldsymbol{k}_f)\right|^2 \tag{12}$$

and the total (or integral) scattering cross section averaged over all directions of incidence

$$\sigma(k) = \frac{1}{4\pi}\int_{4\pi} \mathrm{d}^2\widehat{\boldsymbol{k}}_i \int_{4\pi} \mathrm{d}^2\widehat{\boldsymbol{k}}_f \left|\mathcal{F}(\boldsymbol{k}_i, \boldsymbol{k}_f)\right|^2, \tag{13}$$

may be found. It is to be noticed that the total cross section $\sigma(k)$ may be also obtained from the scattering amplitude via the optical theorem, which states that

$$\sigma(k) = \frac{1}{k}\int_{4\pi} \mathrm{d}^2\widehat{\boldsymbol{k}}_i \, \mathrm{Im}\,\mathcal{F}(\boldsymbol{k}_i, \boldsymbol{k}_i). \tag{14}$$

3. Diffraction from an X_4 (T_d-symmetry) structure

3.1. *Theory*

As an example illustrating applications of the zero-range approximation to problems of interest for chemists and molecular physicists in this section we consider scattering of a plane wave from a system of four identical zero-range scatterers fixed at the points

$$\boldsymbol{r}_1 = (+a, +a, +a), \qquad \boldsymbol{r}_2 = (-a, -a, +a), \tag{15a}$$

$$\boldsymbol{r}_3 = (+a, -a, -a), \qquad \boldsymbol{r}_4 = (-a, +a, -a), \tag{15b}$$

respectively (see figure 1). The distance between any two scatterers is

$$|\boldsymbol{r}_n - \boldsymbol{r}_m| = b \equiv 2\sqrt{2}a \quad (n, m = 1, 2, 3, 4,\ n \neq m). \tag{16}$$

It is easy to observe that the scatterers are situated in vertices of a fictitious regular tetrahedron and therefore the target belongs to the T_d-symmetry group. We shall make extensive use of this fact in the following considerations.

In accord with equation (3), the scattered wave is a superposition of waves emerging from individual centers

$$\Phi(\boldsymbol{k}_i, \boldsymbol{r}) = \sum_{n=1}^{4} f_n(\boldsymbol{k}_i)\phi_n(\boldsymbol{r}). \tag{17}$$

Using the group theoretical methods (see any textbook on quantum chemistry or molecular quantum mechanics, e.g., [1,10]), this wave may be decomposed into partial waves forming bases for the irreducible representations of the symmetry group to which the target belongs. It is found that the function (17) gives rise to one a_1 and three t_2 partial waves

$$\Phi(\boldsymbol{k}_i, \boldsymbol{r}) = \Phi_{a_1}(\boldsymbol{k}_i, \boldsymbol{r}) + \Phi_{t_2,x}(\boldsymbol{k}_i, \boldsymbol{r}) + \Phi_{t_2,y}(\boldsymbol{k}_i, \boldsymbol{r}) + \Phi_{t_2,z}(\boldsymbol{k}_i, \boldsymbol{r}), \tag{18}$$

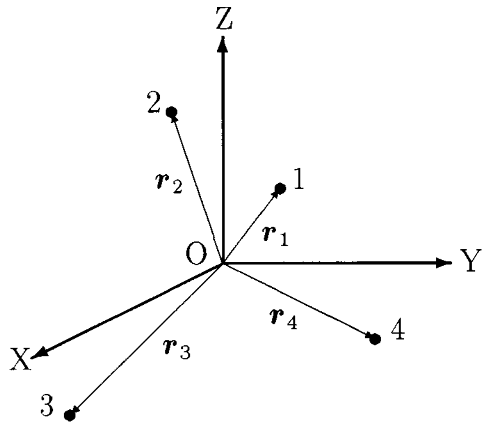

Figure 1. The system of four identical zero-range scatterers forming a T_d-symmetry structure. The scatterers, depicted here of necessity using bullets, are point-like.

where

$$\Phi_{a_1}(\boldsymbol{k}_i,\boldsymbol{r}) = \frac{1}{4}\big[f_1(\boldsymbol{k}_i)+f_2(\boldsymbol{k}_i)+f_3(\boldsymbol{k}_i)+f_4(\boldsymbol{k}_i)\big] \times \big[\phi_1(\boldsymbol{r})+\phi_2(\boldsymbol{r})+\phi_3(\boldsymbol{r})+\phi_4(\boldsymbol{r})\big], \tag{19a}$$

$$\Phi_{t_2,x}(\boldsymbol{k}_i,\boldsymbol{r}) = \frac{1}{4}\big[f_1(\boldsymbol{k}_i)-f_2(\boldsymbol{k}_i)+f_3(\boldsymbol{k}_i)-f_4(\boldsymbol{k}_i)\big] \times \big[\phi_1(\boldsymbol{r})-\phi_2(\boldsymbol{r})+\phi_3(\boldsymbol{r})-\phi_4(\boldsymbol{r})\big], \tag{19b}$$

$$\Phi_{t_2,y}(\boldsymbol{k}_i,\boldsymbol{r}) = \frac{1}{4}\big[f_1(\boldsymbol{k}_i)-f_2(\boldsymbol{k}_i)-f_3(\boldsymbol{k}_i)+f_4(\boldsymbol{k}_i)\big] \times \big[\phi_1(\boldsymbol{r})-\phi_2(\boldsymbol{r})-\phi_3(\boldsymbol{r})+\phi_4(\boldsymbol{r})\big], \tag{19c}$$

$$\Phi_{t_2,z}(\boldsymbol{k}_i,\boldsymbol{r}) = \frac{1}{4}\big[f_1(\boldsymbol{k}_i)+f_2(\boldsymbol{k}_i)-f_3(\boldsymbol{k}_i)-f_4(\boldsymbol{k}_i)\big] \times \big[\phi_1(\boldsymbol{r})+\phi_2(\boldsymbol{r})-\phi_3(\boldsymbol{r})-\phi_4(\boldsymbol{r})\big]. \tag{19d}$$

The coefficients $f_n(\boldsymbol{k}_i)$ may be found from the system of equations (8). In the particular case of the structure discussed in the present section, this system has the form

$$\begin{pmatrix} \mathrm{i}k+\kappa & \mathrm{e}^{\mathrm{i}kb}/b & \mathrm{e}^{\mathrm{i}kb}/b & \mathrm{e}^{\mathrm{i}kb}/b \\ \mathrm{e}^{\mathrm{i}kb}/b & \mathrm{i}k+\kappa & \mathrm{e}^{\mathrm{i}kb}/b & \mathrm{e}^{\mathrm{i}kb}/b \\ \mathrm{e}^{\mathrm{i}kb}/b & \mathrm{e}^{\mathrm{i}kb}/b & \mathrm{i}k+\kappa & \mathrm{e}^{\mathrm{i}kb}/b \\ \mathrm{e}^{\mathrm{i}kb}/b & \mathrm{e}^{\mathrm{i}kb}/b & \mathrm{e}^{\mathrm{i}kb}/b & \mathrm{i}k+\kappa \end{pmatrix} \begin{pmatrix} f_1(\boldsymbol{k}_i) \\ f_2(\boldsymbol{k}_i) \\ f_3(\boldsymbol{k}_i) \\ f_4(\boldsymbol{k}_i) \end{pmatrix} = \begin{pmatrix} -\mathrm{e}^{\mathrm{i}\boldsymbol{k}_i\cdot\boldsymbol{r}_1} \\ -\mathrm{e}^{\mathrm{i}\boldsymbol{k}_i\cdot\boldsymbol{r}_2} \\ -\mathrm{e}^{\mathrm{i}\boldsymbol{k}_i\cdot\boldsymbol{r}_3} \\ -\mathrm{e}^{\mathrm{i}\boldsymbol{k}_i\cdot\boldsymbol{r}_4} \end{pmatrix}. \tag{20}$$

Solving this system directly for $f_n(\boldsymbol{k}_i)$ is not necessary. Indeed, what we really need are the specific linear combinations of the coefficients which appear in equations (19a) to (19d). Adding and subtracting equations from the system (20), one readily finds that

$$\begin{aligned} &f_1(\boldsymbol{k}_i)+f_2(\boldsymbol{k}_i)+f_3(\boldsymbol{k}_i)+f_4(\boldsymbol{k}_i) \\ &\quad= -b\frac{\sqrt{16\pi[1+3(\sin kb)/kb]}}{(\kappa b+3\cos kb)+\mathrm{i}(kb+3\sin kb)}\mathcal{Y}_{a_1}(\boldsymbol{k}_i), \end{aligned} \tag{21a}$$

$$\begin{aligned} &f_1(\boldsymbol{k}_i)-f_2(\boldsymbol{k}_i)+f_3(\boldsymbol{k}_i)-f_4(\boldsymbol{k}_i) \\ &\quad= -\mathrm{i}b\frac{\sqrt{16\pi[1-(\sin kb)/kb]}}{(\kappa b-\cos kb)+\mathrm{i}(kb-\sin kb)}\mathcal{Y}_{t_2,x}(\boldsymbol{k}_i), \end{aligned} \tag{21b}$$

$$\begin{aligned} &f_1(\boldsymbol{k}_i)-f_2(\boldsymbol{k}_i)-f_3(\boldsymbol{k}_i)+f_4(\boldsymbol{k}_i) \\ &\quad= -\mathrm{i}b\frac{\sqrt{16\pi[1-(\sin kb)/kb]}}{(\kappa b-\cos kb)+\mathrm{i}(kb-\sin kb)}\mathcal{Y}_{t_2,y}(\boldsymbol{k}_i), \end{aligned} \tag{21c}$$

$$\begin{aligned} &f_1(\boldsymbol{k}_i)+f_2(\boldsymbol{k}_i)-f_3(\boldsymbol{k}_i)-f_4(\boldsymbol{k}_i) \\ &\quad= -\mathrm{i}b\frac{\sqrt{16\pi[1-(\sin kb)/kb]}}{(\kappa b-\cos kb)+\mathrm{i}(kb-\sin kb)}\mathcal{Y}_{t_2,z}(\boldsymbol{k}_i), \end{aligned} \tag{21d}$$

where

$$\mathcal{Y}_{a_1}(\boldsymbol{k}) = \frac{1}{\sqrt{16\pi[1+3(\sin kb)/kb]}}\left[\mathrm{e}^{\mathrm{i}\boldsymbol{k}\cdot\boldsymbol{r}_1}+\mathrm{e}^{\mathrm{i}\boldsymbol{k}\cdot\boldsymbol{r}_2}+\mathrm{e}^{\mathrm{i}\boldsymbol{k}\cdot\boldsymbol{r}_3}+\mathrm{e}^{\mathrm{i}\boldsymbol{k}\cdot\boldsymbol{r}_4}\right], \tag{22a}$$

$$\mathcal{Y}_{t_2,x}(\boldsymbol{k}) = \frac{-\mathrm{i}}{\sqrt{16\pi[1-(\sin kb)/kb]}}\left[\mathrm{e}^{\mathrm{i}\boldsymbol{k}\cdot\boldsymbol{r}_1}-\mathrm{e}^{\mathrm{i}\boldsymbol{k}\cdot\boldsymbol{r}_2}+\mathrm{e}^{\mathrm{i}\boldsymbol{k}\cdot\boldsymbol{r}_3}-\mathrm{e}^{\mathrm{i}\boldsymbol{k}\cdot\boldsymbol{r}_4}\right], \tag{22b}$$

$$\mathcal{Y}_{t_2,y}(\boldsymbol{k}) = \frac{-\mathrm{i}}{\sqrt{16\pi[1-(\sin kb)/kb]}}\left[\mathrm{e}^{\mathrm{i}\boldsymbol{k}\cdot\boldsymbol{r}_1}-\mathrm{e}^{\mathrm{i}\boldsymbol{k}\cdot\boldsymbol{r}_2}-\mathrm{e}^{\mathrm{i}\boldsymbol{k}\cdot\boldsymbol{r}_3}+\mathrm{e}^{\mathrm{i}\boldsymbol{k}\cdot\boldsymbol{r}_4}\right], \tag{22c}$$

$$\mathcal{Y}_{t_2,z}(\boldsymbol{k}) = \frac{-\mathrm{i}}{\sqrt{16\pi[1-(\sin kb)/kb]}}\left[\mathrm{e}^{\mathrm{i}\boldsymbol{k}\cdot\boldsymbol{r}_1}+\mathrm{e}^{\mathrm{i}\boldsymbol{k}\cdot\boldsymbol{r}_2}-\mathrm{e}^{\mathrm{i}\boldsymbol{k}\cdot\boldsymbol{r}_3}-\mathrm{e}^{\mathrm{i}\boldsymbol{k}\cdot\boldsymbol{r}_4}\right]. \tag{22d}$$

Let us look somewhat closer at properties of the functions (22a) to (22d) which in the description of scattering from the T_d-symmetry obstacle considered here play the same role as the spherical harmonics $Y_{l,m_l}(\widehat{\boldsymbol{k}})$ do in an analysis of scattering from a spherically symmetric target. Firstly, one notices that the functions are normalized to unity in the sense of

$$\int_{4\pi} \mathrm{d}^2\widehat{\boldsymbol{k}}\,\mathcal{Y}^*_{a_1}(\boldsymbol{k})\mathcal{Y}_{a_1}(\boldsymbol{k}) = 1, \tag{23a}$$

$$\int_{4\pi} \mathrm{d}^2\widehat{\boldsymbol{k}}\,\mathcal{Y}^*_{t_2,\alpha}(\boldsymbol{k})\mathcal{Y}_{t_2,\alpha}(\boldsymbol{k}) = 1 \quad (\alpha = x,y,z). \tag{23b}$$

Secondly, it may be verified by direct integration that the functions are mutually orthogonal

$$\int_{4\pi} \mathrm{d}^2\widehat{\boldsymbol{k}}\,\mathcal{Y}^*_{a_1}(\boldsymbol{k})\mathcal{Y}_{t_2,\alpha}(\boldsymbol{k}) = 0 \quad (\alpha = x,y,z), \tag{24a}$$

$$\int_{4\pi} \mathrm{d}^2\widehat{\boldsymbol{k}}\,\mathcal{Y}^*_{t_2,\alpha}(\boldsymbol{k})\mathcal{Y}_{t_2,\alpha'}(\boldsymbol{k}) = 0 \quad (\alpha,\alpha' = x,y,z,\ \alpha\neq\alpha'). \tag{24b}$$

Moreover, in the limiting case when the distance between individual scatterers is very small compared to the wave length, $kb \ll 1$, the function $\mathcal{Y}_{a_1}(\boldsymbol{k})$ becomes the $l = 0$ spherical harmonic

$$\mathcal{Y}_{a_1}(\boldsymbol{k}) \stackrel{kb\to 0}{\longrightarrow} Y_{0,0}\big(\widehat{\boldsymbol{k}}\big) = \frac{1}{\sqrt{4\pi}}, \tag{25a}$$

while the functions $\mathcal{Y}_{t_2,\alpha}(\boldsymbol{k})$, $\alpha = x, y, z$, tend to simple linear combinations of the $l = 1$ spherical harmonics

$$\mathcal{Y}_{t_2,x}(\boldsymbol{k}) \stackrel{kb\to 0}{\longrightarrow} -\frac{1}{\sqrt{2}}Y_{1,+1}\big(\widehat{\boldsymbol{k}}\big) + \frac{1}{\sqrt{2}}Y_{1,-1}\big(\widehat{\boldsymbol{k}}\big) = \sqrt{\frac{3}{4\pi}}\,\widehat{\boldsymbol{k}}\cdot\widehat{\boldsymbol{x}}, \tag{25b}$$

$$\mathcal{Y}_{t_2,y}(\boldsymbol{k}) \stackrel{kb\to 0}{\longrightarrow} \frac{\mathrm{i}}{\sqrt{2}}Y_{1,+1}\big(\widehat{\boldsymbol{k}}\big) + \frac{\mathrm{i}}{\sqrt{2}}Y_{1,-1}\big(\widehat{\boldsymbol{k}}\big) = \sqrt{\frac{3}{4\pi}}\,\widehat{\boldsymbol{k}}\cdot\widehat{\boldsymbol{y}}, \tag{25c}$$

$$\mathcal{Y}_{t_2,z}(\boldsymbol{k}) \stackrel{kb\to 0}{\longrightarrow} Y_{1,0}\big(\widehat{\boldsymbol{k}}\big) = \sqrt{\frac{3}{4\pi}}\,\widehat{\boldsymbol{k}}\cdot\widehat{\boldsymbol{z}}, \tag{25d}$$

where $\widehat{\boldsymbol{x}}$, $\widehat{\boldsymbol{y}}$, $\widehat{\boldsymbol{z}}$ are the unit vectors in the direction of the OX, OY and OZ Cartesian coordinate axes, respectively. (The definition of the spherical harmonics used in the present work follows the Condon–Shortley phase convention [3,4].)

We define the partial scattering amplitudes $\mathcal{F}_{a_1}(\boldsymbol{k}_i, \boldsymbol{k}_f)$ and $\mathcal{F}_{t_2,\alpha}(\boldsymbol{k}_i, \boldsymbol{k}_f)$, $\alpha = x, y, z$, through the asymptotic relations

$$\Phi_{a_1}(\boldsymbol{k}_i, \boldsymbol{r}) \stackrel{r\to\infty}{\longrightarrow} \mathcal{F}_{a_1}(\boldsymbol{k}_i, \boldsymbol{k}_f)\frac{\mathrm{e}^{\mathrm{i}kr}}{r}, \tag{26a}$$

$$\Phi_{t_2,\alpha}(\boldsymbol{k}_i, \boldsymbol{r}) \stackrel{r\to\infty}{\longrightarrow} \mathcal{F}_{t_2,\alpha}(\boldsymbol{k}_i, \boldsymbol{k}_f)\frac{\mathrm{e}^{\mathrm{i}kr}}{r} \quad (\alpha = x, y, z). \tag{26b}$$

Then, it is the consequence of equations (9), (18), (26a) and (26b) that the total scattering amplitude $\mathcal{F}(\boldsymbol{k}_i, \boldsymbol{k}_f)$ may be decomposed in the following way:

$$\mathcal{F}(\boldsymbol{k}_i, \boldsymbol{k}_f) = \mathcal{F}_{a_1}(\boldsymbol{k}_i, \boldsymbol{k}_f) + \sum_{\alpha=x,y,z} \mathcal{F}_{t_2,\alpha}(\boldsymbol{k}_i, \boldsymbol{k}_f). \tag{27}$$

From equations (10), (19a)–(19d) and (21a)–(21d) one infers that angular dependences of the partial scattering amplitudes may be factored out. One has

$$\mathcal{F}_{a_1}(\boldsymbol{k}_i, \boldsymbol{k}_f) = 4\pi F_{a_1}(k)\mathcal{Y}^*_{a_1}(\boldsymbol{k}_f)\mathcal{Y}_{a_1}(\boldsymbol{k}_i), \tag{28a}$$

$$\mathcal{F}_{t_2,\alpha}(\boldsymbol{k}_i, \boldsymbol{k}_f) = 4\pi F_{t_2}(k)\mathcal{Y}^*_{t_2,\alpha}(\boldsymbol{k}_f)\mathcal{Y}_{t_2,\alpha}(\boldsymbol{k}_i) \quad (\alpha = x, y, z), \tag{28b}$$

where the scalar partial amplitudes $F_{a_1}(k)$ and $F_{t_2}(k)$ are

$$F_{a_1}(k) = -\frac{1}{k}\frac{kb + 3\sin kb}{(\kappa b + 3\cos kb) + \mathrm{i}(kb + 3\sin kb)}, \tag{29a}$$

$$F_{t_2}(k) = -\frac{1}{k}\frac{kb - \sin kb}{(\kappa b - \cos kb) + \mathrm{i}(kb - \sin kb)}. \tag{29b}$$

The latter amplitudes may be used to define the scattering phase shifts $\delta_{a_1}(k)$ and $\delta_{t_2}(k)$ through the relations

$$F_{a_1}(k) = \frac{1}{k}\,\frac{1}{\cot\delta_{a_1}(k) - \mathrm{i}}, \qquad F_{t_2}(k) = \frac{1}{k}\,\frac{1}{\cot\delta_{t_2}(k) - \mathrm{i}}, \tag{30}$$

hence, it follows that

$$\cot\delta_{a_1}(k) = -\frac{\kappa b + 3\cos kb}{kb + 3\sin kb}, \qquad \cot\delta_{t_2}(k) = -\frac{\kappa b - \cos kb}{kb - \sin kb}. \tag{31}$$

Once the scattering amplitude has been found, the integral cross section may be found either from equation (13) or from equation (14). In either case one readily obtains

$$\sigma(k) = \sigma_{a_1}(k) + \sigma_{t_2}(k) = \sigma_{a_1}(k) + \sum_{\alpha=x,y,z} \sigma_{t_2,\alpha}(k) \tag{32}$$

with partial cross sections

$$\sigma_{a_1}(k) = \frac{4\pi}{k^2}\sin^2\delta_{a_1}(k) = \frac{4\pi}{k^2}\,\frac{(kb + 3\sin kb)^2}{(\kappa b + 3\cos kb)^2 + (kb + 3\sin kb)^2}, \tag{33a}$$

$$\sigma_{t_2,\alpha}(k) = \frac{4\pi}{k^2}\sin^2\delta_{t_2}(k) = \frac{4\pi}{k^2}\,\frac{(kb - \sin kb)^2}{(\kappa b - \cos kb)^2 + (kb - \sin kb)^2} \quad (\alpha = x, y, z). \tag{33b}$$

Notice that the three t_2 partial waves contribute equally to the total cross section.

3.2. Discussion

We begin the discussion of the results of section 3.1 with analyzing the phase shifts $\delta_{a_1}(k)$ and $\delta_{t_2}(k)$. Their values, extracted from equation (31), are plotted in figure 2 against kb for six representative values of the product κb. Since equation (31) defines the phase shifts modulo π only, we have normalized $\delta_{a_1}(k)$ and $\delta_{t_2}(k)$ so that they vanish at $kb = 0$. It is seen that both phase shifts show an oscillatory dependence on kb. The phase $\delta_{a_1}(k)$ goes through $-\pi/2$ at such values of kb, denoted henceforth as $k_{a_1}b$, that

$$\cos k_{a_1}b = -\frac{1}{3}\kappa b, \quad -3 < \kappa b < 3, \tag{34}$$

while the phase $\delta_{t_2}(k)$ crosses $+\pi/2$ at $kb = k_{t_2}b$ such that

$$\cos k_{t_2}b = \kappa b, \quad -1 < \kappa b < 1. \tag{35}$$

It is known from the general theory of wave scattering [11] that resonant features occur in a partial cross section around such wave numbers for which the corresponding phase shift goes across an odd multiple of $\pi/2$ and, simultaneously, the partial wave retardation stretch, defined by Wigner [13] as

$$\Delta L = 2\frac{\mathrm{d}\delta(k)}{\mathrm{d}k}, \tag{36}$$

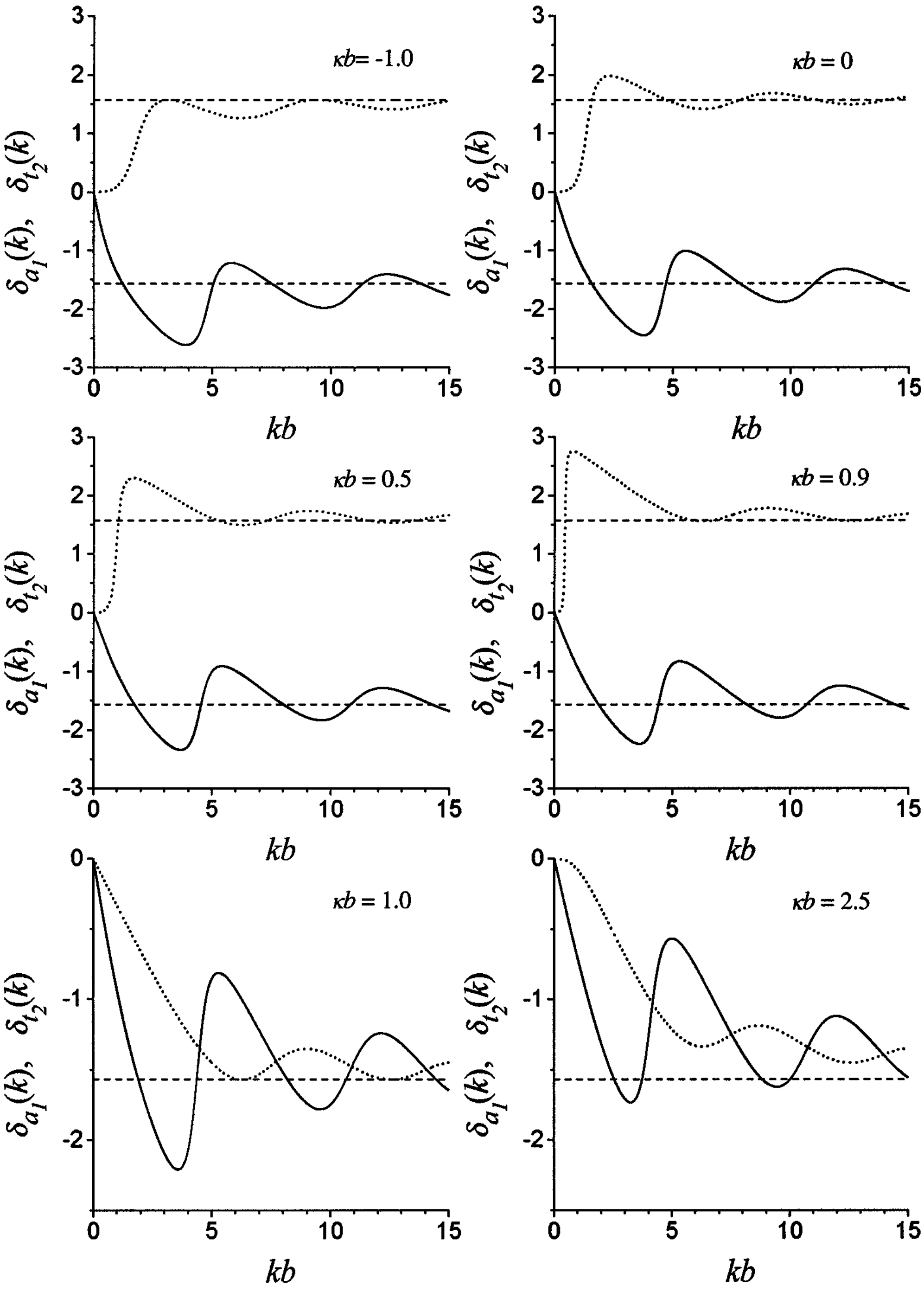

Figure 2. The phase shifts $\delta_{a_1}(k)$ (the solid line) and $\delta_{t_2}(k)$ (the dotted line) plotted versus kb for six representative values of the parameter κb. The horizontal dashed lines have been drawn at $\pm\pi/2$.

exceeds a characteristic dimension L of the region where a wave interacts with a target. Applying this result to the present case we see that resonances in the a_1 and t_2 partial waves will occur around the roots of equations (34) and (35), respectively, provided that

$$\frac{2}{b}\frac{\mathrm{d}\delta_{a_1}(k)}{\mathrm{d}k}\bigg|_{k=k_{a_1}} > 1 \quad \text{and} \quad \frac{2}{b}\frac{\mathrm{d}\delta_{t_2}(k)}{\mathrm{d}k}\bigg|_{k=k_{t_2}} > 1, \tag{37}$$

respectively. By evaluating the derivatives, the conditions (37) are transformed to the forms

$$-2\frac{3\sin k_{a_1}b}{k_{a_1}b+3\sin k_{a_1}b} > 1 \quad \text{and} \quad 2\frac{\sin k_{t_2}b}{k_{t_2}b-\sin k_{t_2}b} > 1, \tag{38}$$

respectively. The inequalities (38) may be solved either graphically or numerically. It is found that the first of them is satisfied for

$$\xi_{a_1}^{(1)} < k_{a_1}b < \xi_{a_1}^{(2)}, \tag{39}$$

where

$$\xi_{a_1}^{(1)} \simeq 3.547, \qquad \xi_{a_1}^{(2)} \simeq 5.610 \tag{40}$$

are two lowest positive roots of

$$\frac{\sin\xi}{\xi} = -\frac{1}{9}, \tag{41}$$

while the second is satisfied for

$$0 < k_{t_2}b < \xi_{t_2}^{(1)}, \tag{42}$$

where

$$\xi_{t_2}^{(1)} \simeq 2.279 \tag{43}$$

is the lowest positive root of

$$\frac{\sin\xi}{\xi} = \frac{1}{3}. \tag{44}$$

On combining these results with equations (34) and (35), one concludes that a resonance, located around

$$k_{a_1}b = \pi + \arccos\frac{1}{3}\kappa b, \tag{45}$$

arises in the partial wave a_1 for

$$-2.346 < \kappa b < 2.757, \tag{46}$$

while a resonance in the partial wave t_2, located around

$$k_{t_2}b = \arccos\kappa b, \tag{47}$$

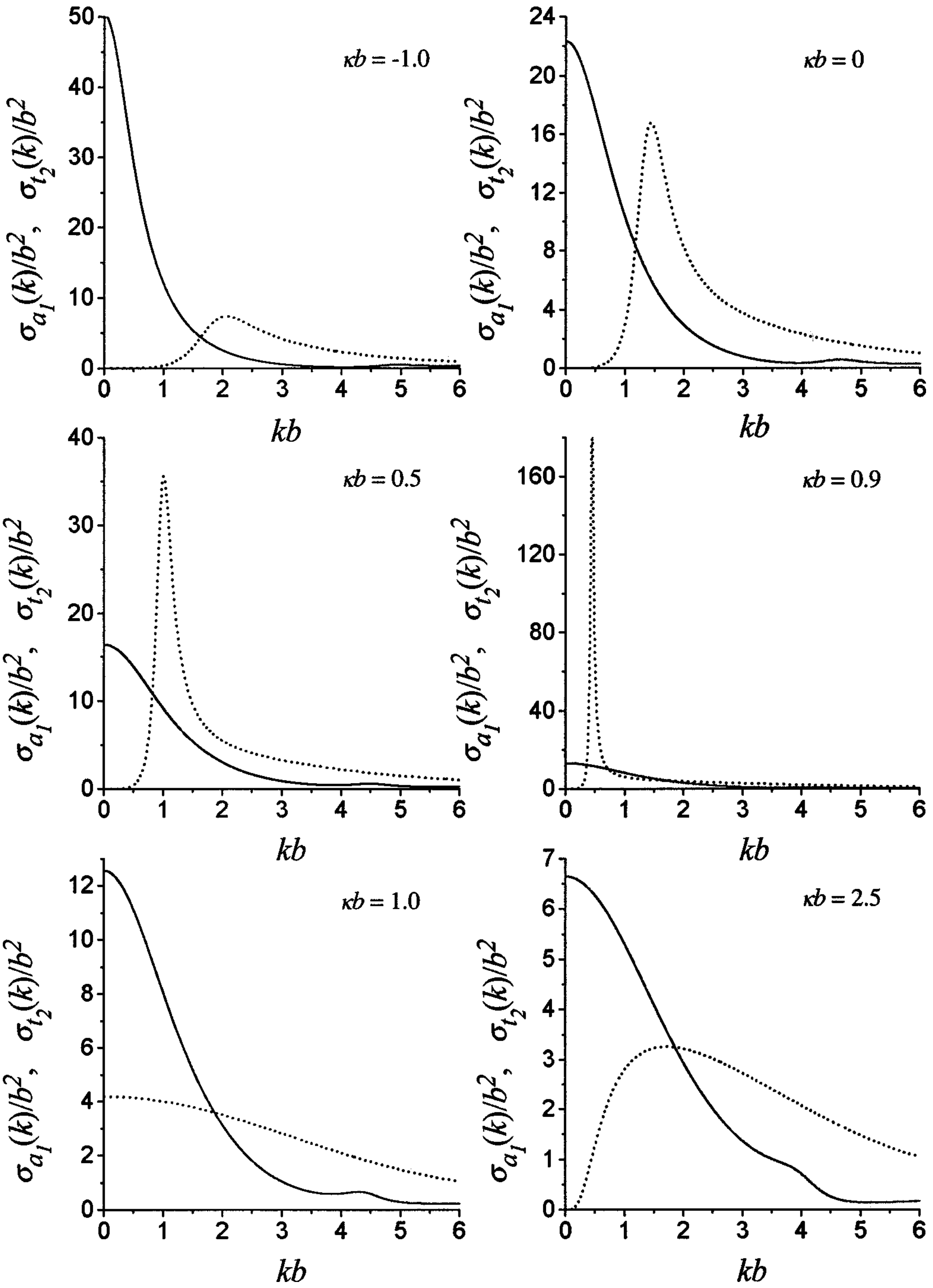

Figure 3. The partial cross sections $\sigma_{a_1}(k)$ (the solid line) and $\sigma_{t_2}(k)$ (the dotted line) plotted versus kb for the same values of the parameter κb as used in figure 2.

occurs for

$$-0.650 < \kappa b < 1. \tag{48}$$

In equations (45) and (47) the principal branch of the arc cosine is used.

We now pass on to analysis of the partial cross sections $\sigma_{a_1}(k)$ and $\sigma_{t_2}(k)$ plotted against kb in figure 3. The resonance predicted in the $\delta_{t_2}(k)$ phase shift at low values of kb manifests itself as a pronounced peak in the corresponding partial cross section $\sigma_{t_2}(k)$. As the product κb tends towards the unity from below, the peak becomes higher, narrower and its position shifts towards very small values of kb. For $\kappa b \geqslant 1$ the resonant peak disappears and the observed maximum is of nonresonant origin. The limiting case $\kappa b = 1$ is exceptional since only in this case the partial cross section $\sigma_{t_2}(k)$ does not vanish for $k = 0$; instead, it takes there the value $4\pi b^2/3$. The shape of the curve $\sigma_{a_1}(k)$ differs distinctly from $\sigma_{t_2}(k)$ and the a_1-resonance is seen only as a low broad hump in $\sigma_{a_1}(k)$ located as predicted by equation (45).

Acknowledgements

This work was supported in part by the Polish State Committee for Scientific Research under grants No. 228/P03/99/17 and 215/P03/99/17.

References

[1] P.W. Atkins, *Molecular Quantum Mechanics* (Oxford University Press, Oxford, 1970) Chapter 5.
[2] J.M. Blatt and V.F. Weisskopf, *Theoretical Nuclear Physics* (Wiley, New York, 1952) Section 2.3.C.
[3] E.U. Condon and G.H. Shortley, *The Theory of Atomic Spectra* (Cambridge University Press, Cambridge, 1935) Section 3.4.
[4] R.D. Cowan, *The Theory of Atomic Structure and Spectra* (University of California Press, Berkeley, CA, 1981) Section 2.5.
[5] Yu.N. Demkov and V.N. Ostrovskii, *Zero-Range Potentials and Their Applications in Atomic Physics* (Leningrad University Press, Leningrad, 1975) (in Russian, English translation: Plenum, New York, 1988).
[6] Yu.N. Demkov and V.S. Rudakov, Zh. Eksp. Teor. Fiz. 59 (1970) 2035.
[7] G.F. Drukarev, Adv. Quantum Chem. 11 (1978) 251.
[8] G.F. Drukarev, *Collisions of Electrons with Atoms and Molecules* (Nauka, Moscow, 1978) (in Russian, English translation: Plenum, New York, 1987) Sections 1.4 and 1.7.
[9] K. Huang, *Statistical Mechanics* (Wiley, New York, 1963) Sections 13.2, 13.3 and appendix B.
[10] Ch.S. Johnson and L.G. Pedersen, *Problems and Solutions in Quantum Chemistry and Physics* (Dover, New York, 1986) Appendix 8.
[11] R.G. Newton, *Scattering Theory of Waves and Particles*, 2nd ed. (Springer, New York, 1982) Section 11.2.
[12] R. Szmytkowski and Cz. Szmytkowski, Phys. Lett. A 235 (1997) 217. (In the second of equations (23) of that work the subscript Σ_g should be replaced by Σ_u; in equation (25) the second equality symbol should be replaced by the multiplication symbol.)
[13] E.P. Wigner, Phys. Rev. 98 (1955) 145.